Title: The short-term acquisition of a skill learning task unveils the neural filtering of shared synaptic input to spinal motor neurons

Abbreviated title: Common synaptic alterations with skill learning

Authors:
Hélio V. Cabral[1], Alessandro Cudicio[1], Alberto Bonardi[1], Alessandro Del Vecchio[2], Luca Falciati[1], Claudio Orizio[1], Eduardo Martinez-Valdes[3], Francesco Negro[1*]

Affiliations:
[1]Department of Clinical and Experimental Sciences, Università degli Studi di Brescia, 25123, Brescia, Italy
[2]Department Artificial Intelligence in Biomedical Engineering, Friedrich-Alexander University, 91052, Erlangen, Germany
[3]School of Sport, Exercise and Rehabilitation Sciences, College of Life and Environmental Sciences, University of Birmingham, B152TT, Birmingham, UK

*Corresponding author email:
francesco.negro@unibs.it

Number of pages: 41
Number of figures: 6
Number of tables: 2
Number of words (Abstract): 250
Number of words (Introduction): 724
Number of words (Discussion): 2004

Conflict of interest statement: The authors declare no competing financial interests.

Acknowledgments: This study was funded by the European Research Council Consolidator Grant INcEPTION (contract no. 101045605).

Abstract

Skill acquisition of force-matching tasks is mediated by adaptations of spinal and supraspinal pathways to alpha motoneurons. In this study, we estimated the shared synaptic contributions of these pathways to understand the neural mechanisms behind the short-term acquisition of a new force-matching task. High-density surface electromyography (HDsEMG) was acquired from the first dorsal interosseous (FDI; 7 males and 6 females) and tibialis anterior (TA; 7 males and 4 females) while participants performed 15 trials of an isometric force-matching task. For two selected trials (pre- and post-skill acquisition), we decomposed the HDsEMG into motor unit spike trains, tracked motor units between trials, and calculated the mean discharge rate and the coefficient of variation of inter-spike interval (CoV_{ISI}). We also quantified the ratio (post/pre) of the area under the curve of motor units' coherence within delta, alpha, and beta bands. For both muscles, improvements in force-matching were accompanied by a significant increase in the mean discharge rate and a decrease in CoV_{ISI}. In addition, the area under the curve within the alpha band significantly decreased by ~22% and ~13% for the TA and FDI muscles, respectively, with no changes in the delta or beta bands. Our results indicate that the short-term acquisition of a new force-matching skill is mediated by the attenuation of shared synaptic noise oscillations unrelated to the target force fluctuations. In other words, the central nervous system acts as a matched filter to modulate the synaptic weights of shared inputs and suppress neural components unrelated to the specific task.

Keywords: motor unit, common synaptic input, force control, skill learning

Significance statement

Previous studies have proposed that only the low-frequency oscillations of shared synaptic inputs to the motor neurons, encompassing voluntary and involuntary components, are responsible for the generated muscle force. In our study, we investigated whether the acquisition of a new motor task involving precise force generation requires specific alterations in these shared synaptic inputs components. Our findings demonstrated that, for both a hand muscle and a leg muscle, the skill acquisition was mediated by a reduction in shared synaptic oscillations unrelated to the required force fluctuations. Therefore, during the learning of a force-matching task, the central nervous system acts like a neural filter, modulating the synaptic weights of shared inputs to attenuate neural components unrelated to the specific task.

Introduction

Over the past three decades, the measurement of incremental motor skill acquisition has emerged as a relevant experimental paradigm for investigating the cognitive and neural processes underlying the learning of new motor abilities (Karni et al., 1998; Ungerleider et al., 2002). Initially, the new movement is produced with varying accuracy, but with repetition and practice, the central nervous system refines the movement, resulting in effortless and precise execution (Willingham, 1998). Consequently, the learning of a new motor task entails structural and functional alterations in the supraspinal and spinal pathways (i.e., neural plasticity) to accommodate the acquisition and retention of skilled motor behaviors (Ungerleider et al., 2002; Dayan and Cohen, 2011). Indeed, compelling evidence from studies on primates (Plautz et al., 1995; Nudo et al., 1996) and non-primates (Kleim et al., 1998) animals have demonstrated that, following motor skill training, there is an expansion of the cortical representations related to the trained task. Similar neural adaptations have been observed in humans in studies using non-invasive imaging and neurophysiological techniques (Karni et al., 1995; Pascual-Leone et al., 1995; Perez et al., 2004; Jensen et al., 2005). Specifically, the acquisition of new motor skills has been shown to significantly increase cortical representation (Karni et al., 1995; Pascual-Leone et al., 1995; Pascual-Leone et al., 1999) and corticospinal excitability (Perez et al., 2004; Jensen et al., 2005) of the muscles involved in the training task. While there is greater consensus regarding the effects of motor skill learning on supraspinal adaptations in humans, the dynamics of plastic changes in synaptic connectivity to spinal motor neurons remain relatively unexplored in the literature.

Many daily activities require the rapid acquisition of motor tasks that demand precise control of fine movements within short time intervals (Johansson and Westling, 1988). As the generation of precise movements relies on the accurate modulation of muscle forces (Johansson

and Westling, 1988; Kumar et al., 2017), specific control strategies are necessary during motor skill learning to overcome the inherent variability of the neural pathways innervating muscles. Interestingly, previous research has demonstrated that the motor neuron pool behaves as a very selective filter, eliminating components of synaptic input that are not common to all motor neurons (Negro and Farina, 2011a; Farina et al., 2014; Negro et al., 2016a). Additionally, it has also been observed that the muscle itself acts as a spatial and temporal smoothing filter of the neural drive (Bawa and Stein, 1976; Baldissera et al., 1998), further minimizing the effects of independent sources of neural synaptic noise across the alpha motor neuron pools. Collectively, these investigations indicate that only the low-frequency components of the synaptic inputs widely shared across the motor neuron pools are represented in the force output (Enoka and Farina, 2021). In voluntary tasks, these shared or common synaptic inputs consist of voluntary components related to the intentional control of the task (e.g., control input signals from cortico-spinal pathways) and involuntary components that act as noise oscillations reducing the precision of the task (e.g., physiological tremor from spinal and supraspinal pathways). Thus, learning new motor tasks involving precise force generation should require minimizing these shared noise components unrelated to the intended motor task in order to maximize the representation of shared synaptic input related to voluntary control in the force output. Even though this hypothesis appears intuitively correct, no study has yet experimentally addressed this issue.

Therefore, the present study aimed to investigate whether the short-term acquisition of a new force-matching skill is mediated by alterations in the shared synaptic input to spinal motor neurons. We hypothesized that the acquisition of a new motor skill in an individual muscle would require specific adaptations in the neural pathways to the motor neuron pool of that muscle, ultimately reducing the contributions of shared synaptic oscillations unrelated to the

target force fluctuations. In other words, during the acquisition of a force-matching task, the central nervous system may tune the synaptic weights of the spinal and supraspinal projections to the motor neuron pool to create a matched filter that suppresses the neural components unrelated to the specific intended task. We experimentally tested this hypothesis by decomposing high-density surface electromyograms from the first dorsal interosseous (FDI) and tibialis anterior (TA) muscles during the learning of a complex, isometric force-matching task. In addition, we conducted simulations of entire motor neuron pools to elucidate the neural mechanisms that could explain our results.

Materials and Methods

Participants

Twenty-four healthy volunteers participated in the study. Specifically, two experiments were performed in which 13 participants (6 females; age: 31 ± 4 years; height: 176.8 ± 7.1 cm; mass: 71.9 ± 16.4 kg) had the FDI tested, and 11 (4 females; age: 31 ± 3 years; height: 174.9 ± 9.0 cm; mass: 71.2 ± 18.1 kg) the TA muscle. All participants were free from musculoskeletal or neurological injuries and provided written informed consent prior to the beginning of experiments. This study was approved by the local ethics committee (code NP5665) and conformed to the latest Declaration of Helsinki.

Experimental design

Participants took part in a single experimental session lasting ~1h. For the measurements on the FDI muscle, participants sat on an adjustable chair with their elbow flexed at 45° (0° being the anatomical position) and their right upper arm and hand comfortably resting on a custom-made device. The wrist and the hand were in a neutral position. The middle phalanx of the index finger was fixed to an adjustable support attached to a load cell (SM-100 N, Interface, Arizona, USA) so that the isometric abduction force produced by the index finger could be measured (**Figure 1A**). To standardize the hand position and minimize the contribution of other muscles, the little, ring, and middle fingers were separated from the index finger and secured to the device with Velcro straps. The forearm was also strapped to the device, and the thumb was secured at ~80° angle to the index finger (**Figure 1A**). For the measurements on the TA muscle, participants were comfortably seated on a custom-built ankle dynamometer with their right knee fully extended, their ankle at 10° of plantar flexion (0° being the foot perpendicular to the shank), and their hip flexed at 70° (0° being the hip fully extended). The right foot was fixed with Velcro straps to an adjustable footplate perpendicularly connected to a load cell

(SM-500 N, Interface, Arizona, USA) to record the dorsiflexion isometric force produced by the ankle (**Figure 1B**).

For both TA and FDI muscles, participants were initially asked to perform three isometric maximal voluntary contractions (MVCs) for 3 s, with a 60 s interval of rest in between. The greatest value across the three MVCs was considered the maximal isometric force and used as a reference for the following submaximal contractions. Then, after 5 min rest period, participants were instructed to perform 15 trials of a complex, isometric force-matching task (force-matching skill acquisition). The task involved a linear increase in force at a rate of 5% MVC/s, a variable force region for 30 s, and a linear decrease in force at a rate of 5% MVC/s. The variable force region contained oscillations above and below the target force level (averaged exerted force), which was defined as 5% MVC for the FDI and 10% MVC for the TA. The level of 5% MVC was chosen for the FDI to minimize fatigue effects across the task. Specifically, the oscillations consisted of a randomly generated signal with frequency content below 1.5 Hz (-3 dB low pass frequency). Two trajectories were generated, one for each muscle (**Figure 1C**), and the same trajectory was used throughout all trials and for all the subjects (Knight and Kamen, 2004). Each trajectory consisted of a black line, depicting the target force, over a white background and a red line depicting the subject's force. A minimum of 60 s of rest was provided between trials, and prior to each trial, participants were encouraged by the same investigator to follow the target as closely as possible. Visual feedback from the target and the force was displayed on a computer monitor positioned at ~60 cm in front of the participant, in which the entire target trajectory was visible and stationary.

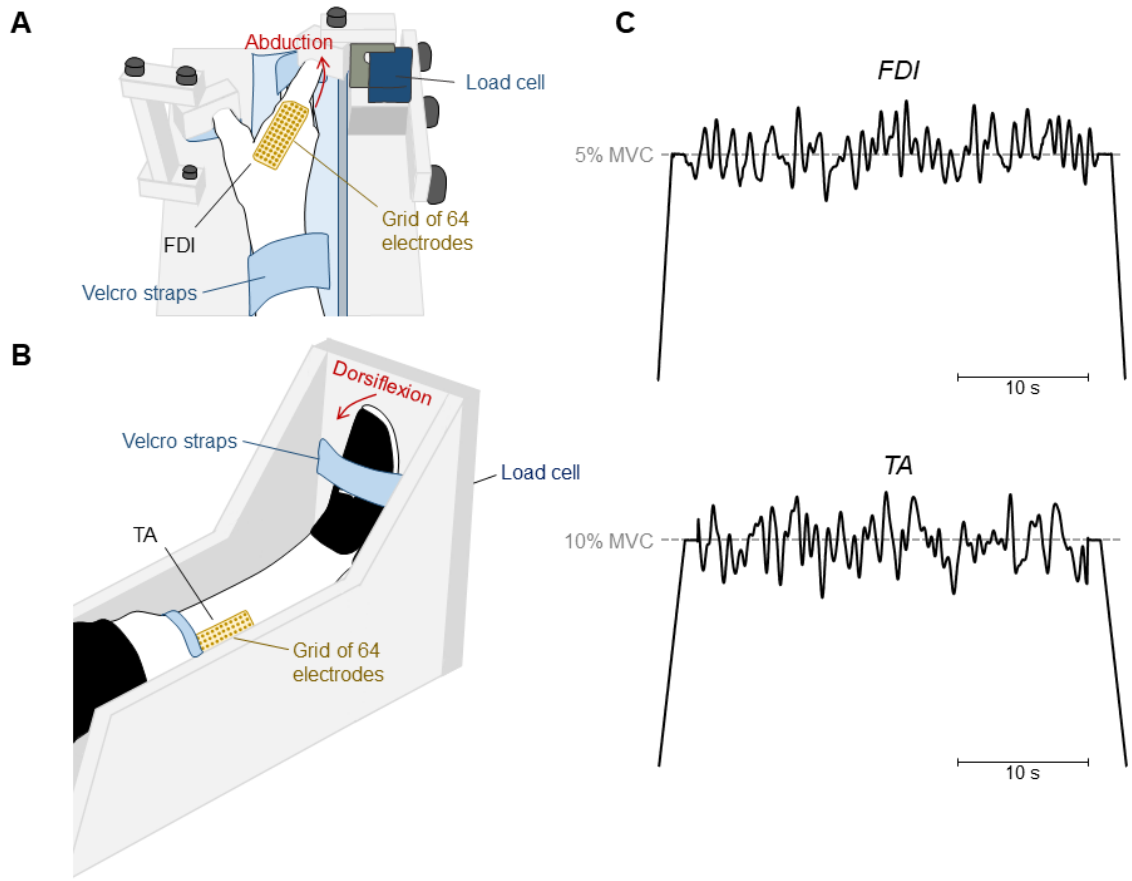

Figure 1: Experimental setup. *A, position of the participants' wrist and hand on the custom-made dynamometer to record the abduction isometric force produced by the index finger. B, position of the participants' shank and foot on the custom-built dynamometer to measure the dorsiflexion isometric force produced by the ankle. High-density surface electromyography grids were placed over the first dorsal interosseous (FDI) muscle (A) and tibialis anterior (TA) muscle (B). C, Isometric force-matching tasks presented to the participants for the FDI (top) and the TA (bottom) muscles. Tasks involved a plateau region of 30 s containing a randomly generated signal low-pass filtered at 1.5 Hz. The target force level was defined as 5% and 10% of maximal voluntary contraction for the FDI and TA, respectively. The same trajectory was used throughout all trials of the force-matching skill task.*

Data collection

During all trials of the force-matching task, high-density surface electromyograms (HDsEMG) were acquired from FDI and TA muscles using a grid of 64 electrodes arranged into 13 rows x 5 columns, with a missing electrode on a corner (4 mm inter-electrode distance for FDI; 8 mm

inter-electrode distance for TA; OT Bioelettronica, Turin, Italy). An experienced investigator determined the position and orientation of the grids via palpation of anatomical landmarks. Specifically, the electrodes were attached over the belly of each muscle in the following locations: FDI, lateral to the line connecting the heads of the first and second metacarpals (**Figures 1A**); TA, ~1 cm lateral to the tibial prominence (**Figure 1B**). Electrodes were fixed to the skin using a bi-adhesive foam, and the electrode-skin contact was ensured by filling the foam cavities with conductive paste (AC cream, Spes Medica, Genova, Italy). Reference electrodes were positioned on the right wrist for the FDI and on the right ankle for TA. Prior to electrode placement, the skin was cleaned with an abrasive paste (EVERI, Spes Medica, Genova, Italy) and shaved when necessary. Surface EMGs were recorded in monopolar mode and digitized at 2000 samples/s using a 16-bit wireless amplifier (10-500 Hz bandwidth; Sessantaquattro, OT Bioelettronica, Turin, Italy). Force signals provided by the load cell were amplified by a factor of 100 (Forza-j, OT Bioelettronica, Turin, Italy) and sampled synchronously with EMGs.

Data analysis

Force and HDsEMG signals were analyzed offline using MATLAB custom-written scripts.

Force. First, force signals were low-pass filtered at 15 Hz using a third-order Butterworth filter. Then, to quantify the performance for each trial of the force-matching task, the root-mean-square error (RMSE) between the force and target signals was computed for the middle 30-s of the target (i.e., oscillatory region) (Knight and Kamen, 2004). Cross-correlation peak values were also calculated for the middle 30-s to assess similarities between fluctuations in force and target signals. For both RMSE and cross-correlation analyses, the detrended version of the signals was used. To assess force-matching improvements during the skill acquisition task,

three out of the 15 trials were selected for each participant to represent the *pre-*, *during-* and *post-skill acquisition*. Specifically, the three trials selected were the ones with the highest, average, and smallest RMSE between the force and target signals. The number of selected trials was stored for further analysis. In addition, to quantify how force steadiness changed during the learning task, we calculated the coefficient of variation (i.e., standard deviation/mean) of detrended force signals for the three selected trials.

Identification and tracking of motor units. For simplicity, we considered only the *pre-* and *post-skill acquisition* trials for all motor unit analyses. Moreover, similarly to the force, all analyses were performed for the middle 30-s of the target (i.e., oscillatory region). First, HDsEMG signals were bandpass filtered with a third-order Butterworth filter (20-500 Hz cut-off frequencies). After visual inspection, channels with low signal-to-noise ratio or artifacts were discarded. Then, the HDsEMG signals were decomposed into motor unit spike trains using a convolutive blind-source separation algorithm (Negro et al., 2016b). This method has been previously validated and extensively applied to assess the activity of single motor units (Castronovo et al., 2015; Negro et al., 2016b; Cogliati et al., 2020; Hassan et al., 2020). After the automatic identification of motor units, all the motor unit spike trains were visually inspected for false positives or false negatives (Hassan et al., 2020). Missing pulses or incorrectly assigned pulses producing non-physiological discharge rates were manually and iteratively edited by an experienced operator, and motor unit spike trains were re-estimated as previously proposed (Martinez-Valdes et al., 2017; Hassan et al., 2020). This approach has been shown to be highly reliable across operators (Hug et al., 2021). After the editing of motor unit spike trains, the motor units were tracked between the *pre-* and *post-skill acquisition* trials. This was achieved by reapplying the motor unit separation vectors, which are estimated with the blind source separation algorithm, from one trial to the other (Oliveira and Negro, 2021;

Rossato et al., 2022). These motor unit separation vectors are unique for each individual motor unit and define the spatio-temporal matched filters to estimate the motor unit spike trains. This tracking procedure was performed in the forward and backward directions (i.e., motor unit separation vectors of *pre-skill acquisition* trial were applied on the *post-skill acquisition* trial, and vice-versa). Thus, our approach ensured that the same motor units were tracked and analyzed in both trials. Only motor units spike trains with a silhouette value, which is a metric to assess decomposition accuracy (Negro et al., 2016b), higher than 0.8 were used for analysis (Kapelner et al., 2020). For three participants in FDI and one participant in TA, we tracked the motor units based on their shape (Martinez-Valdes et al., 2017), as we were not able to track at least four motor units (see *Estimates of common synaptic input*) by reapplying the motor unit separation vectors. For this analysis, the two-dimensional representations of the motor unit action potentials of the identified motor units in the *pre-skill acquisition* trial were cross-correlated with the two-dimensional representations of the identified motor units in the *post-skill acquisition* trial (Martinez-Valdes et al., 2017; Cogliati et al., 2020). Only motor units with highly similar motor unit action potentials (cross-correlation > 0.8) were considered as belonging to the same motor units. The mean discharge rate and coefficient of variation of inter-spike interval (COV_{ISI}) were calculated for each matched motor unit and stored for further analysis.

Estimates of common synaptic input. To assess changes in common synaptic input to motor neurons with the force-matching skill acquisition, coherence analysis was performed between cumulative spike trains (CST) of motor units from the same muscle (Negro and Farina, 2012; Castronovo et al., 2015; Negro et al., 2016a; Maillet et al., 2022; Rossato et al., 2022). Coherence is a frequency-domain linear coupling measure between two signals. This analysis was performed on two equally sized CSTs comprising motor units randomly selected from the

identified, matched units. The number of motor units selected for each of the two groups was half of the total number of detected units, and this was repeated for up to 100 permutations. Only participants with at least four matched motor units were included in the coherence analysis. For all permutations, coherence was calculated between the two detrended CSTs using Welch's periodogram with a 1-s Hanning window and an overlap of 95%. The obtained values were averaged for all permutations and transformed into standard z-scores as described by Gallet and Julien (2011). Only z-scores greater than the bias were considered for further analysis. The bias was determined as the mean value, for frequencies higher than 5 Hz, of z-score profiles estimated from the shuffled version of motor unit spike trains, as no significant coherence is expected in this case. To evaluate changes between *pre-* and *post-skill acquisition* trials, the areas under the curve of the z-coherence profiles within the delta (1-5 Hz), alpha (5-15 Hz) and beta (15-35 Hz) bands were calculated, and then, the area under the curve ratio (*post/pre*) was computed separately for each bandwidth. We subtracted one from the values of the area under the curve ratio so that values higher and lower than 0 indicated, respectively, an increase and decrease in z-coherence during *post-* compared to *pre-skill acquisition* trial. For purposes of visualization only, the pooled z-coherence across all participants was calculated as previously proposed (Baker et al., 2003).

Signal-to-noise ratio analysis. To indirectly assess changes in voluntary and involuntary synaptic inputs with the force-matching skill acquisition, we calculated the signal-to-noise ratio (SNR) between the target template and the force, and between the target template and neural drive to muscles. In both cases, an increase in SNR values between *pre-* and *post-skill acquisition* trials would indicate a decrease in the common synaptic oscillations unrelated to the intended motor task (i.e., a reduction in the involuntary synaptic components). For this analysis, the neural drive to the muscles was estimated by summing the binary discharge trains

across all identified motor units (i.e., CST) (Thompson et al., 2018) and normalized by the number of active motor units during the contraction. For the normalization procedure, an index indicating when each motor unit was active was calculated as done previously (Mazzo et al., 2021), and the indices for all motor units were summed to obtain a total index of active motor units. Before calculating the SNR, the target, force, and CST signals, were low-pass filtered at 5 Hz using a fourth-order Butterworth filter.

Simulations

To elucidate the neural mechanisms that could explain our results, we simulated populations of motor neurons (Cisi and Kohn, 2008) that received common and independent inputs in varying relative proportions (Negro and Farina, 2012). Detailed descriptions of the modelling approach adopted can be found in previous studies (Negro and Farina, 2011b; Farina et al., 2014; Negro et al., 2016a). The motor neuron parameters were the same as those used by Cisi and Kohn (2008) and were selected according to an exponential distribution over the pool of motor neurons (Fuglevand et al., 1993).

The number of motor neurons was set to 450, of which ~270 were fully recruited (discharge rate > 6 pulses per second (pps); (Farina et al., 2014)). The input to the motor neuron pool was modelled as a linear summation of common synaptic input to all motor neurons and an independent noise input specific to each motor neuron (Negro et al., 2016a). The common synaptic input, which represents the input originating from the brain stem, spinal interneurons, or muscle afferents, includes a voluntary synaptic component and an involuntary synaptic component. In our simulations, the voluntary component (i.e., common drive) was simulated using the same random signal provided as the target to the participants during the skill acquisition task in the TA experimental recordings. The involuntary synaptic components (e.g.,

physiological tremor and others) were simulated as a band-limited (15 Hz) Gaussian noise. Finally, the independent noise input, which represents the individual variability of the membrane potential of each motor neuron, was modeled as a Gaussian noise with a bandwidth of 50 Hz (Negro et al., 2016a).

Based on our main hypothesis, two different models were created to simulate the *pre-skill acquisition* and *post-skill acquisition* trials. For each model, ten realizations of signal noise were performed. For each realization, the standard deviation of the involuntary synaptic input for the *post-skill acquisition* model was set to be half of the one defined for the *pre-skill acquisition* model (i.e., simulating a reduction in the involuntary synaptic input with the force-matching skill acquisition). The simulated force output obtained for each realization was retained for further analysis. The models were implemented in MATLAB (The MathWorks Inc., Natick, Massachusetts, USA). For purposes of visualization, we calculated the area under the curve of the simulated synaptic input power spectrum (voluntary and involuntary components) for each realization. To assess changes in common synaptic input between the two simulated models (*pre-skill acquisition* and *post-skill acquisition*), we calculated the ratio (*post/pre*) of the area under the curve of coherence within delta (1-5 Hz), alpha (5-15 Hz) and beta (15-35 Hz) bands. Moreover, to examine whether the simulated reduction in involuntary synaptic input was a determinant to improvements in force-matching, we calculated the RMSE between the simulated force output and the target template and compared the results between the two models (*pre-skill acquisition* and *post-skill acquisition*). The RMSE was calculated as described for the experimental data.

Statistical analysis

All statistical analyses were performed in R (version 4.3.0), using RStudio environment (version 2023.03.1).

To compare the RMSE, cross-correlation peak values and coefficient of variation of force between *pre-*, *during-* and *post-skill acquisition* trials, Friedman tests were used. When significant effect of 'trial' was detected, post-hoc tests with Bonferroni correction were conducted for pairwise comparisons. The Wilcoxon signed-rank test was used to compare RMSE values between the *pre-skill acquisition* and *post-skill acquisition* models.

To compare mean discharge rate and COV_{ISI} between *pre-* and *post-skill acquisition* trials, linear mixed-effect models (LMM) were applied, as they allow for the inclusion of all detected units and not just the mean value for each participant and trial (Boccia et al., 2019). Specifically, this statistical model accounts for the non-independence of observations, which is particularly useful for this experimental design due to the hierarchical nature of motor unit data (greater correlation for units within participants compared to between participants; (Tenan et al., 2014)). For both mean discharge rate and COV_{ISI}, random intercept models were applied with 'trial' (*pre-* and *post-skill acquisition*) as fixed effect and 'participant' as random effect (e.g., *mean discharge rate ~ 1 + trial + (1 | participant)*). LMMs were implemented using the package *lmerTest* (Kuznetsova et al., 2017) with the Kenward-Roger method to approximate the degrees of freedom and estimate the *p*-values. The *emmeans* package was used to determine estimated marginal means and their differences with 95% confidence intervals (Lenth et al., 2019).

For both experimental and simulated data, to compare estimates of common synaptic input (i.e., coherence) between *pre-* and *post-skill acquisition* trials, changes in area under the curve

ratio (*post/pre*) were tested using one-sample Wilcoxon signed-rank test ($\mu_0 = 0$), separately for delta, alpha and beta bands. In addition, Spearman correlations were performed for the experimental data to test whether differences in area under the curve between trials were associated with differences in mean discharge rate between trials, separately for each muscle. For this analysis, the mean discharge rate of motor units was averaged within participants, and the ratio between *pre-* and *post-skill acquisition* trials (*post/pre*) was calculated. To compare the SNR values between *pre-* and *post-skill acquisition* trials, Wilcoxon signed-rank tests were used.

For all statistical comparisons, statistical significance was set at an α of 0.05. For the results of motor unit discharge properties, the values in the text are reported as mean with 95% confidence intervals. All the other values are reported as mean ± standard deviation in the text and median/interquartile ranges in the figures. All individual data of motor unit discharge times are available at https://doi.org/10.6084/m9.figshare.23703804.

Results

Improvements in force-matching during skill acquisition task

To assess improvements in force-matching during the skill acquisition task, we compared the RMSE and cross-correlation peak values between the force and target signals on the three selected trials out of the 15. While for the TA muscle, the trials selected to represent *pre*-, *during*- and *post-skill acquisition* were, on average, the second, the fifth, and the twelfth, respectively, for the FDI muscle were the first, the fourth, and the thirteenth. **Figure 2A** shows the fluctuations in dorsiflexion isometric force produced by a representative participant for the three selected trials. Improvements in force-matching are visually evident across trials, which is confirmed by a decrease of ~43% in RMSE (from 1.16 to 0.66 %MVC) and an increase of ~88% in cross-correlation peak value (from 0.41 to 0.78) when comparing *post*- with *pre-skill acquisition*. Similar results were obtained for group data. For both TA and FDI muscles, there were significant differences in RMSE ($P < 0.001$ for both muscles, Friedman test) and cross-correlation peak values ($P < 0.001$ for both muscles, Friedman test) among trials. Specifically, for both muscles, RMSE values were significantly lower *during* and *post* compared to *pre-skill acquisition* trial, with a significant reduction also observed between *during* and *post* ($P < 0.003$ for all, Bonferroni post-hoc test; **Figures 2B** and **2C**). Moreover, for both muscles, cross-correlation peak values obtained *during* and *post* trials were significantly greater than *pre-skill acquisition* trial, with significantly greater values also observed for *post* than *during* ($P < 0.003$ for all, Bonferroni post-hoc tests; **Figures 2D** and **2E**).

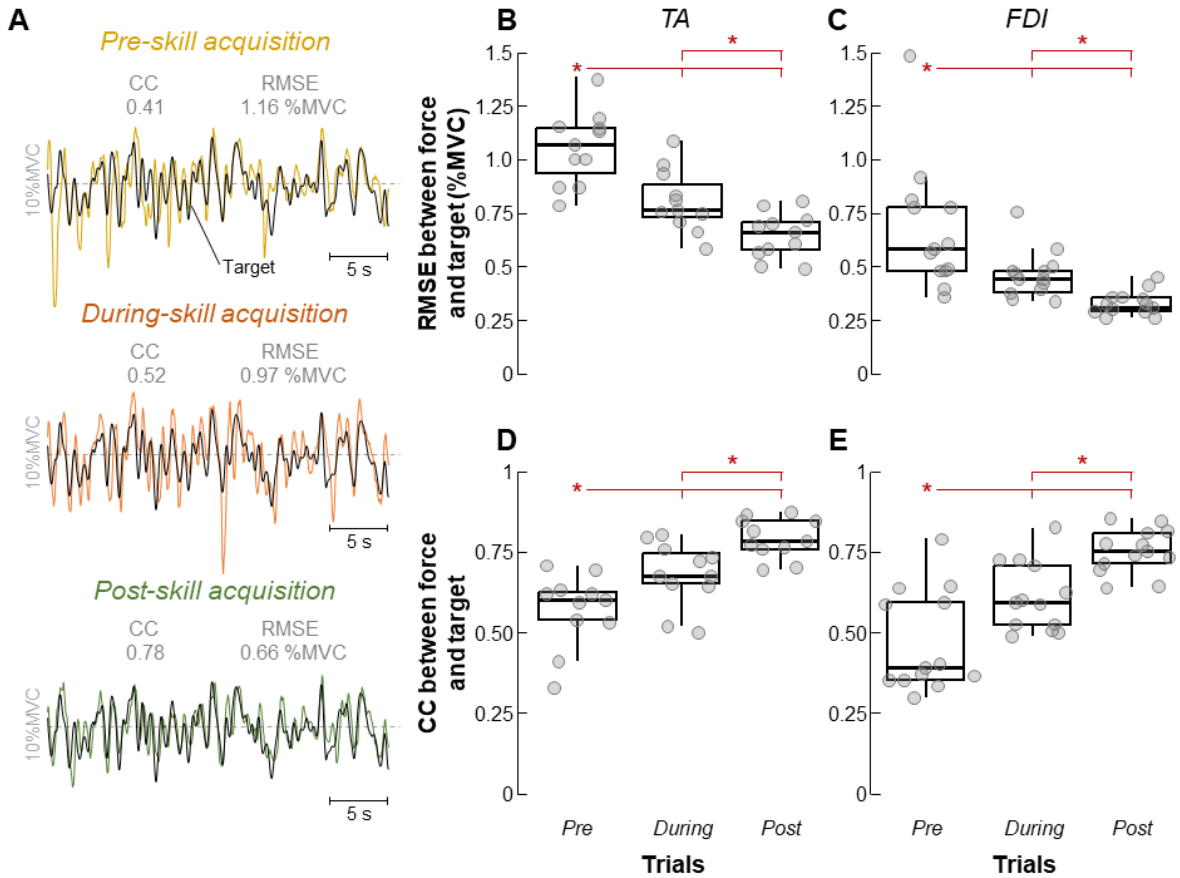

Figure 2: Performance results. *Three out of the 15 trials were selected for each participant to represent the pre-, during- and post-skill acquisition trials. A, Representative comparison between the force and target during the skill acquisition task. The yellow, orange, and green lines indicate dorsiflexion isometric forces produced by a participant for the pre-, during- and post-skill acquisition trials, respectively. The black line indicates the target. B-E, Group results of root-mean-square-error (RMSE) and cross-correlation (CC) between the force and target for the tibialis anterior (TA) muscle (B and D) and the first dorsal interosseous (FDI) muscle (C and E). Gray circles identify individual participants. Horizontal traces, boxes, and whiskers denote median value, interquartile interval, and distribution range. *P<0.05.*

To assess whether the force steadiness changed with the force-matching skill acquisition, we quantified the coefficient of variation of force for the three selected trials. For both TA and FDI muscles, there were significant differences in the coefficient of variation of force among trials ($P < 0.001$ for both muscles; Friedman test). Specifically, the coefficient of variation of

force values obtained for *during* and *post* trials were significantly lower than *pre-skill acquisition* trial for both TA (*pre*: 11.77 ± 1.57%, *during*: 9.97 ± 0.90%, *post*: 9.51 ± 0.83%; $P < 0.015$ for all; Bonferroni post-hoc tests) and FDI (*pre*: 14.13 ± 6.18%, *during*: 10.30 ± 2.20%, *post*: 8.65 ± 0.93%; $P < 0.001$ for all, Bonferroni post-hoc tests) muscles. Additionally, a significant reduction in the coefficient of variation of force was also observed between *during* and *post* for FDI ($P = 0.004$, Bonferroni post-hoc test), but not for TA muscle ($P = 0.442$, Bonferroni post-hoc test).

Changes in motor unit discharge properties with skill acquisition

In order to evaluate changes in motor unit discharge properties (i.e., mean discharge rate and COV_{ISI}) with the force-matching skill acquisition, we decomposed HDsEMG signals into motor unit spike trains. Note that we tracked motor units in *pre-* and *post-skill acquisition* to ensure the same motor units were compared between trials (see *Methods* section for further details). For the TA muscle, we identified a total of 166 and 198 motor units for *pre-* and *post-skill acquisition* trials, respectively, and were able to track 138 motor units (13 ± 7 motor units per participant). For the FDI muscle, instead, we identified a total of 105 and 127 motor units for *pre-* and *post-skill acquisition* trials, respectively, from which 62 were tracked across trials (5 ± 2 motor units per participant). All details regarding the number of motor units identified and tracked for each participant are provided in **Table 1** (TA muscle) and **Table 2** (FDI muscle).

Table 1: Number of motor units identified and matched for the tibialis anterior muscle.

Participants	Pre-skill acquisition trial	Post-skill acquisition trial	Matched motor units
#1	18	22	18
#2	13	17	17
#3	19	22	7
#4	12	8	6

#5	12	13	11
#6	24	24	19
#7	4	9	1
#8	20	20	8
#9	6	5	5
#10	21	31	26
#11	17	27	20
Total	166	198	138
Mean ± std	15 ± 6	18 ± 8	13 ± 7

Table 2: Number of motor units identified and matched for the first dorsal interosseous muscle.

Participants	Pre-skill acquisition trial	Post-skill acquisition trial	Matched motor units
#1	11	14	6
#2	10	14	3
#3	12	13	7
#4	5	10	4
#5	4	6	4
#6	12	11	7
#7	7	7	4
#8	4	5	3
#9	13	12	8
#10	8	10	7
#11	5	6	2
#12	6	12	5
#13	8	7	2
Total	105	127	62
Mean ± std	8 ± 3	10 ± 3	5 ± 2

For both muscles, a significant effect of trial (*pre-* vs *post-skill acquisition*) was found on the mean discharge rate and COV_{ISI} values of matched motor units. Specifically, for the TA muscle, the mean discharge rate significantly increased from 10.9 [9.95, 11.9] to 11.9 [10.92, 12.9] pps between *pre-* and *post-skill acquisition* trials (F = 23.083, P < 0.001, LMM; **Figure 3A**). Conversely, the COV_{ISI} significantly decreased from 48.0 [42.9, 53.2] to 31.4 [26.3, 36.3] % with the force-matching skill acquisition (F = 22.986, P < 0.001, LMM; **Figure 3C**). Similar results were observed for the FDI muscle, with the values of mean discharge rate significantly

increasing from 11.6 [10.5, 12.7] to 12.3 [11.3, 13.4] pps (F = 5.166, P = 0.025, LMM; **Figure 3B**), and the values of COV_{ISI} significantly decreasing from 46.6 [39.4, 53.8] to 35.4 [28.1, 42.6] % (F = 8.952, P = 0.003, LMM; **Figure 3D**) between *pre-* and *post-skill acquisition* trials.

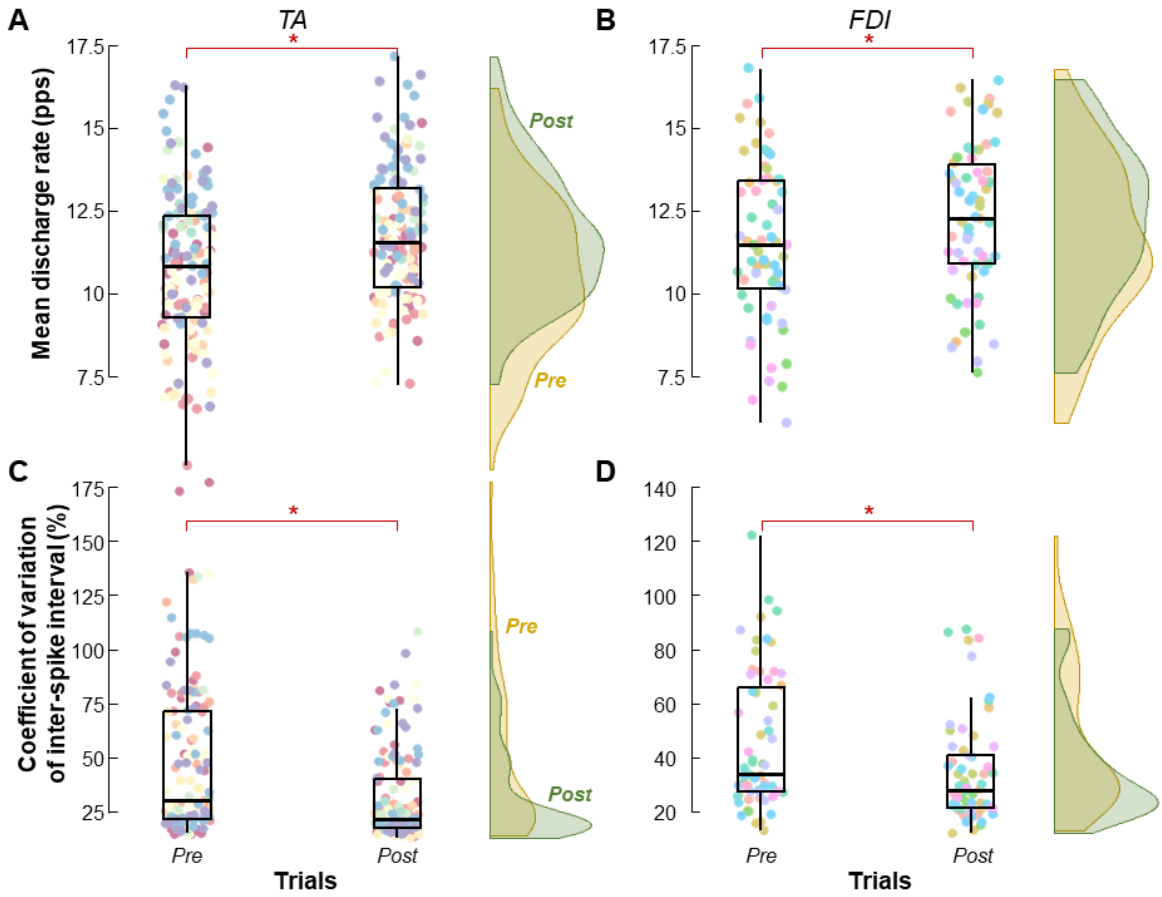

Figure 3: Mean discharge rate and discharge variability results. *A-B, mean discharge rate results of matched motor units between pre- and post-skill acquisition trials for the tibialis anterior (TA) muscle (A) and the first dorsal interosseous (FDI) muscle (B). C-D, coefficient of variation of inter-spike interval results of matched motor units between pre- and post-skill acquisition trials for the TA (C) and FDI (D) muscles. Each circle identifies a matched motor unit between trials. Each color of the circles corresponds to a specific participant. Horizontal traces, boxes, and whiskers denote median value, interquartile interval, and distribution range. Density curves of the data are represented on the right side of each panel by half-violin plots (yellow for pre-skill acquisition and green for post-skill acquisition). Note that density curves can be used to visually compare differences between pre- and post-skill acquisition trials. *P<0.05.*

Changes in common synaptic input with skill acquisition

In order to assess changes in common synaptic input between *pre-* and *post-skill acquisition* trials, we used coherence analysis between the spike trains of matched motor units. We specifically quantified the ratio (*post/pre*) of the area under the curve of z-coherence within delta (1-5 Hz), alpha (5-15 Hz) and beta (15-35 Hz) bands. The coherence analysis was performed in 10 and 9 participants for TA and FDI muscles, respectively, as only three or fewer motor units were matched for participant #7 in TA, and participants #2, #8, #11, and #13 in FDI (see **Tables 1** and **2**). **Figures 4A** and **4B** display the pooled z-coherence for all participants. When comparing *pre-* and *post-skill acquisition* trials, for both TA and FDI muscles there is a clear reduction in the area under the curve in the alpha band (grey area in **Figure 4A** and **4B**). Indeed, for the TA muscle, there was a significant median reduction of ~22% in the area under the curve within the alpha band between *pre-* and *post-skill acquisition* trials (P = 0.014, Wilcoxon signed-rank test; **Figure 4C**), which was not observed either for delta or beta bands (P > 0.322 for both, Wilcoxon signed-rank test). Similarly, for the FDI muscle, the area under the curve within the alpha band significantly decreased by a median of ~13% with the force-matching skill acquisition (P = 0.008, Wilcoxon signed-rank test; **Figure 4D**), but did not significantly change for delta or beta bands (P > 0.074 for both, Wilcoxon signed-rank test).

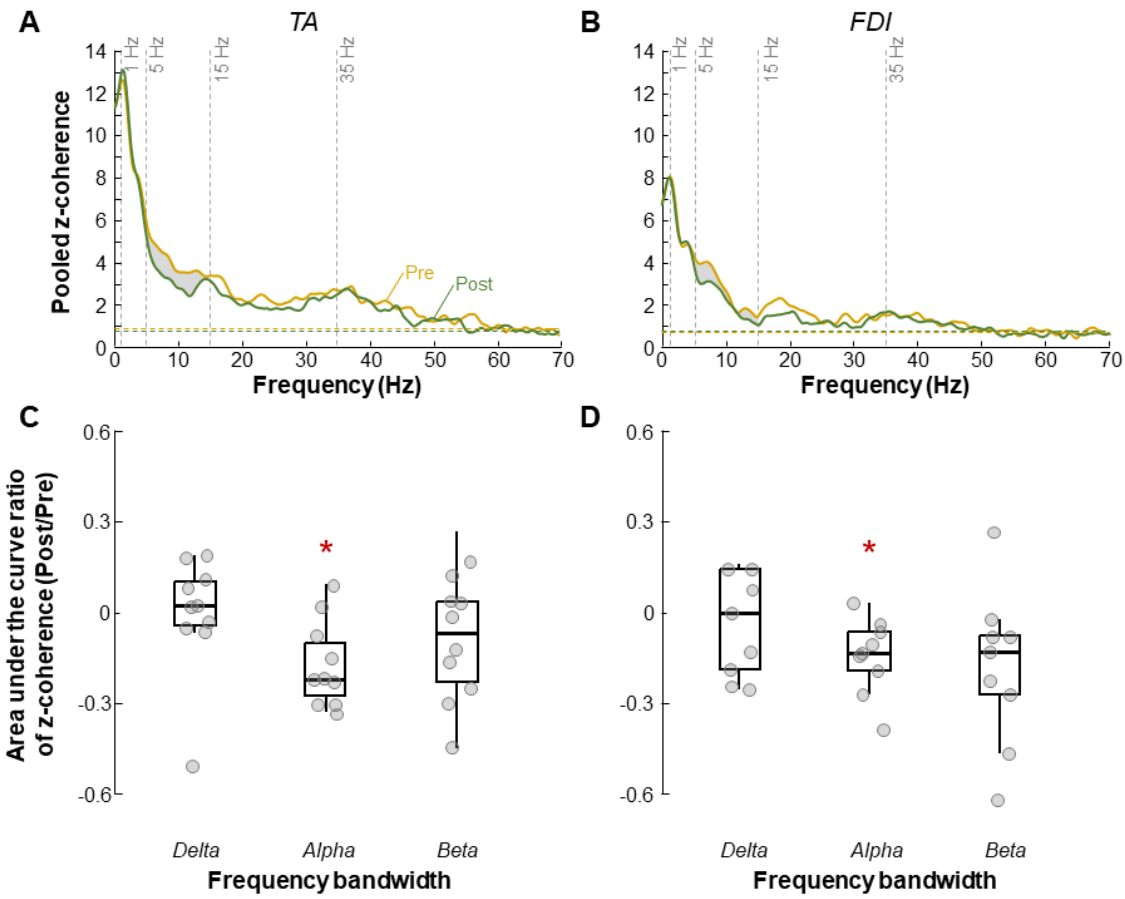

Figure 4: Coherence results. *A-B, pooled z-coherence profiles considering all participants for the tibialis anterior (TA) muscle (A) and first dorsal interosseous (B) muscles (yellow for pre-skill acquisition and green for post-skill acquisition). The horizontal dashed line indicates the confidence level. Vertical dashed lines highlight the three frequency regions analyzed: delta (1-5 Hz), alpha (5-15 Hz), and beta (15-35 Hz) bands. Grey areas denote statistical differences in the area under the curve between pre- and post-skill acquisition trials. C-D, Group results of the area under the curve ratio of coherence for the TA (C) and FDI (D) muscles. Gray circles identify individual participants. Horizontal traces, boxes, and whiskers denote median value, interquartile interval, and distribution range. *P<0.05.*

To investigate whether differences in area under the curve of z-coherence between trials were associated with differences in mean discharge rate between trials, we used Spearman correlations. There were no significant associations for delta (*Spearman's* ρ = 0.33, P = 0.347 for TA; *Spearman's* ρ = 0.63, P = 0.067 for FDI), alpha (*Spearman's* ρ = -0.07, P = 0.855 for

TA; *Spearman's* ρ = 0.02, P = 0.966 for FDI) or beta (*Spearman's* ρ = -0.10, P = 0.777 for TA; *Spearman's* ρ = 0.35, P = 0.356 for FDI) bands.

Signal-to-noise ratio results

To indirectly investigate changes in voluntary and involuntary synaptic inputs between *pre-* and *post-skill acquisition* trials, we computed the SNR between the target and the force, and between the target and the neural drive to the muscles (i.e., smoothed CST). **Figures 5** shows the target oscillation and FDI force fluctuation (panel A) or smoothed CST (panel C) for a representative participant. It is possible to observe that, when compared to the target, the SNR values increased between *pre-* and *post-skill acquisition* trials for both force and CST signals. Like in this representative participant, group data results showed for each muscle a significant increase in the target-force SNR between *pre-* and *post-skill acquisition* trials (P < 0.005 for both cases, Wilcoxon rank-signed test; **Figure 5B**). Similarly, the target-CST SNR values obtained for *post-* were significantly greater than *pre-skill acquisition* for both TA and FDI muscles (P < 0.048 for both cases, Wilcoxon rank-signed test; **Figure 5D**).

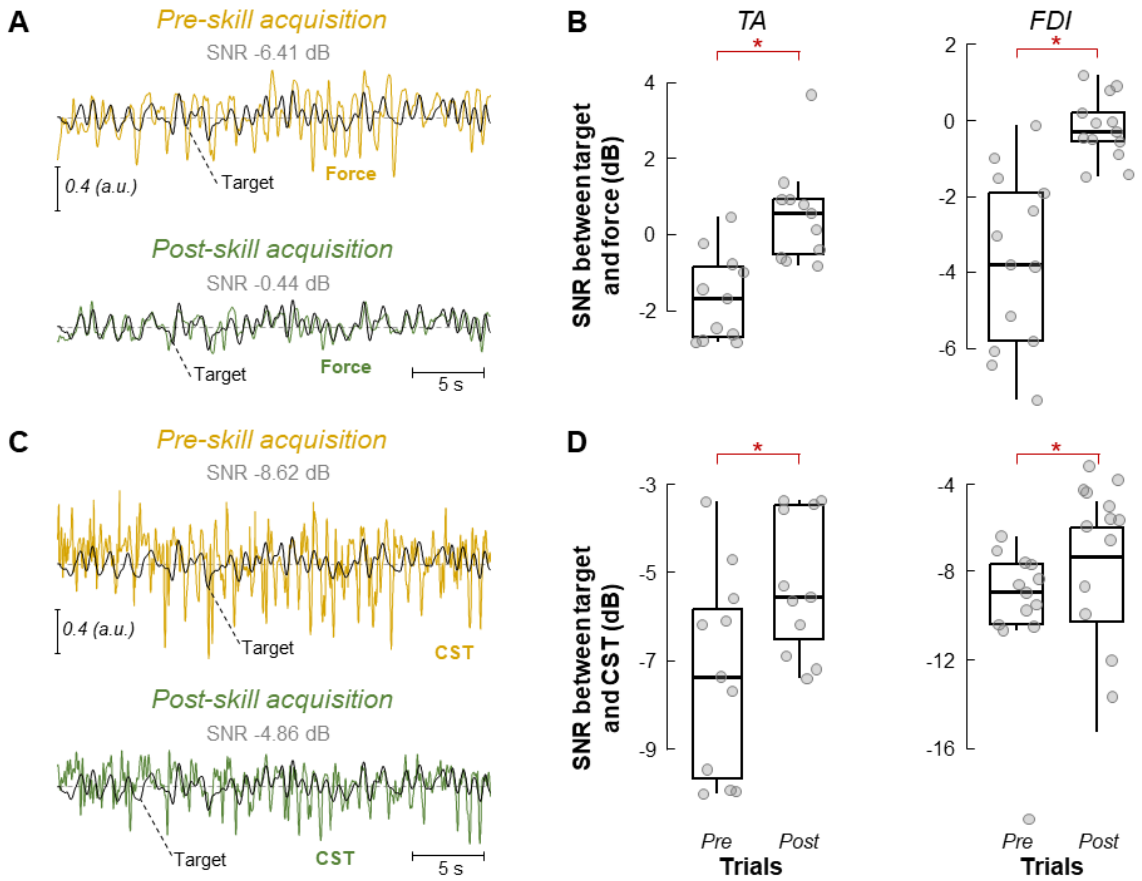

Figure 5: Signal-to-noise ratio results. *Representative participant results of signal-to-noise ratio (SNR) between target and first dorsal interosseous (FDI) force (A), and between target and cumulative spike train (CST) (C). The yellow and green lines denote pre- and post-skill acquisition trials, respectively. Note that for both the force and CST, the signal fluctuations became more similar to the target in the post- compared to pre-skill acquisition trial. B-C, group results of SNR between target and force (B), and between target and CST (C) for the tibialis anterior (TA) muscle (left panel) and FDI (right panel). Gray circles identify individual participants. Horizontal traces, boxes, and whiskers denote median value, interquartile interval, and distribution range. *P<0.05.*

Simulations results

To explore the mechanisms that could explain our results, we simulated a population of motor neurons receiving common and independent inputs (see *Methods* section). We then quantified the ratio (*post/pre*) of the area under the curve of coherence within delta (1-5 Hz), alpha (5-15 Hz) and beta (15-35 Hz) bands. **Figure 6A** depicts an example of a single simulation realization. The top graph shows that while the power spectrum of voluntary synaptic input

(i.e., common drive; 1-5 Hz) was very similar between simulated *pre-* and *post-skill acquisition* trials, there was a clear reduction in the power spectrum of involuntary synaptic input (e.g., physiological tremor and others; 5-15 Hz). Accordingly, the coherence results of this realization showed a reduction in the alpha band, but not in the delta or beta bands.

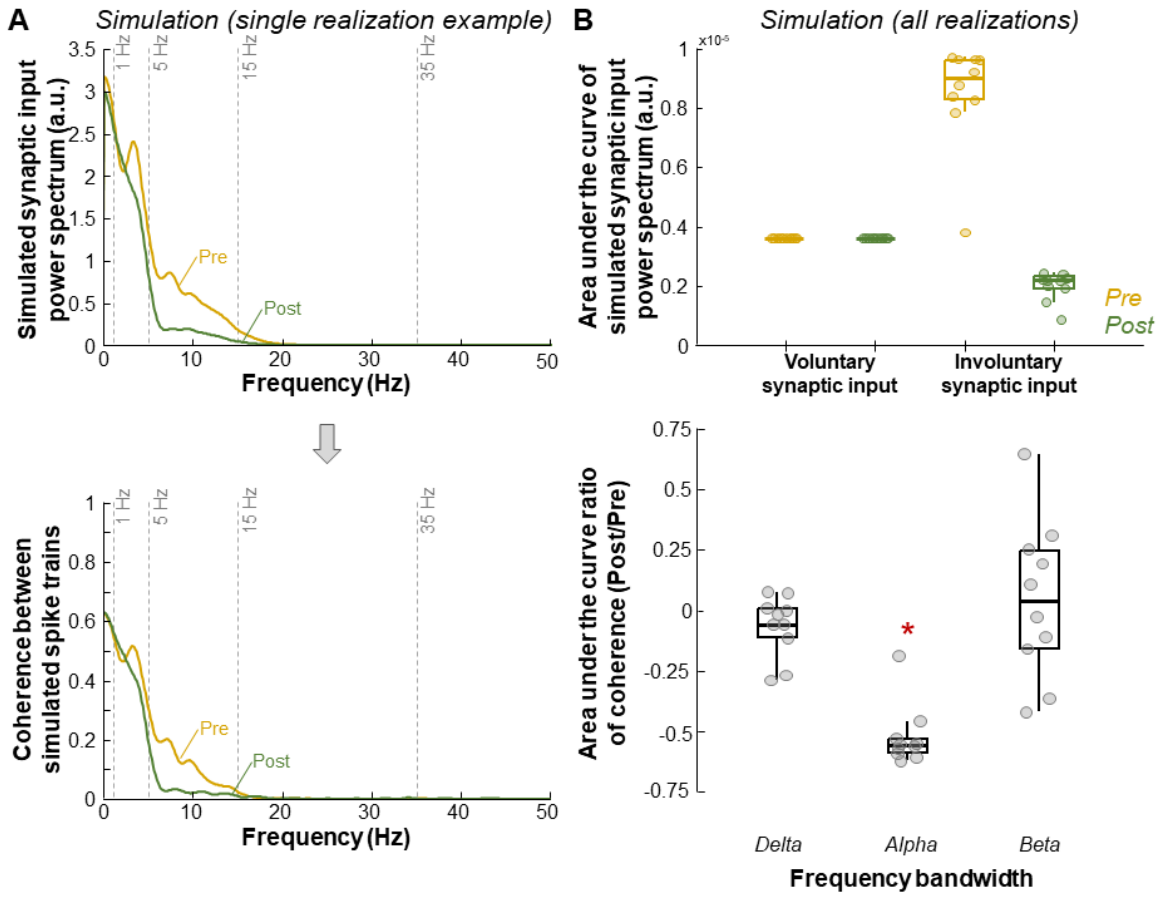

Figure 6: Simulation results. *A, representative case of a single simulation realization. Changes in the power spectrum of simulated synaptic input (top graph) and coherence between simulated spike trains (bottom graph) are shown for the pre- (yellow line) and post-skill acquisition (green line) trials. Vertical dashed lines highlight the three frequency regions analyzed: delta (1-5 Hz), alpha (5-15 Hz), and beta (15-35 Hz) bands. B, results of the area under the curve of simulated synaptic input power spectrum (top graph) and the area under the curve ratio of coherence (bottom graph) for all simulations. Gray circles identify individual simulation realizations. Horizontal traces, boxes, and whiskers denote median value, interquartile interval, and distribution range. a.u., arbitrary unit. *P<0.05.*

Similar results were found from the ten realizations of simulation. The top graph of **Figure 6B** shows that the area under the curve of power spectrum of the voluntary synaptic input was the same between simulated *pre*- and *post-skill acquisition* trials. Instead, when considering the involuntary synaptic input, there was a decrease in the area under the curve of power spectrum between *pre* and *post*. In accordance with the experimental results, the area under the curve of coherence within the alpha band significantly decreased between simulated *pre*- and *post-skill acquisition* trials ($P < 0.002$, Wilcoxon signed-rank test; bottom graph in **Figure 6B**) but did not significantly change either for delta or beta bands ($P > 0.232$ for both; Wilcoxon signed-rank test). To examine the influence of reduced involuntary synaptic input, leading to a decrease in alpha band oscillations, on the force-matching skill acquisition, we compared the RMSE between the force output generated from simulated motor neurons and the target signal in the two models. There was a significant decrease in RMSE values between *pre*- and *post-skill acquisition* models ($P = 0.037$, Wilcoxon signed-rank test).

Discussion

In this study, we investigated whether short-term learning of a complex, isometric force-matching task is mediated by specific adaptations in the shared synaptic inputs to alpha motor neuron pools of the TA and FDI muscles. Our experimental findings revealed that both muscles exhibited improvements in force-matching, accompanied by a reduction in coherent oscillations across motor neuron spike trains unrelated to the required force fluctuations as skill acquisition progressed. These findings were further supported by simulations involving a population of motor neurons receiving common and independent inputs. As discussed below, these outcomes suggest that the acquisition of a new force-matching task involves specific changes in supraspinal and spinal neural circuitry that behave as a matched neural filter, ultimately minimizing shared noise components unrelated to the intended task.

Traditionally, motor sequence learning, which assesses the incremental acquisition of sequential motor skills, has been employed as experimental paradigm to investigate neuroplasticity underlying skilled task acquisition (Karni et al., 1998; Ungerleider et al., 2002). Psychophysiological evidence has revealed that two main stages are involved in this paradigm: a fast stage characterized by considerable performance improvements within a single session, and a slow stage where further but quantitatively smaller improvements can be observed across multiple sessions (Ungerleider et al., 2002; Dayan and Cohen, 2011). Consistent with previous research (Knight and Kamen, 2004; Perez et al., 2005), our study focused on the fast-learning stage of incremental motor skill acquisition, as we aimed to investigate the rapid acquisition of a fine control task involving muscle force modulation. Thus, ensuring that the observed neural plastic changes in this study were specifically related to the force-matching skill task, and did not arise from overall motor activity or other confounding factors, is a necessary step for interpreting our main results. The median reductions in RMSE of ~40% for both the TA and

FDI observed after 15 repetitions of the task, along with cross-correlation increases of ~40% for the TA and ~85% for the FDI (**Figure 2**), indicate that the chosen task and number of trials were sufficiently challenging to enable skill acquisition. Previous experiments employing a similar task involving index finger abduction demonstrated comparable RMSE improvements (~50%) between force and target over the same number of repetitions (Knight and Kamen, 2004). Importantly, significant improvements in force-matching were already evident by the fifth trial for the TA and fourth trial for the FDI (*during-skill acquisition* trial), suggesting an exponential decay pattern in the error curve, which is in agreement with the classical pattern of motor performance improvement during learning (Heathcote et al., 2000). Taking these factors into consideration, it is plausible to assume that the alterations identified in motor unit discharge characteristics and shared synaptic inputs are indeed associated with the intended force-matching task.

Due to the low-pass and amplification characteristics of the motor neuron pool, experimental and simulated data have extensively demonstrated that only the low-frequency components of the synaptic inputs largely shared across the motor neuron pool are represented in the generated muscle force (Negro et al., 2009; Negro and Farina, 2011b, a; Farina et al., 2014; Negro et al., 2016a; Thompson et al., 2018). Thus, the weights of the voluntary and involuntary components of these common synaptic inputs are determinants for precise force modulation (for a review, see Farina and Negro (2015)). Although these components' contributions to the generation of common synaptic input may not be directly measured in humans, they have been indirectly estimated through coherence analysis of discharge times of motor unit spike trains (Negro and Farina, 2012; Castronovo et al., 2015; Maillet et al., 2022; Rossato et al., 2022). For instance, Castronovo et al. (2015) have shown significant coherence between motor unit spike trains up to ~80 Hz during sustained isometric contractions, and these results have been repeatedly

confirmed by several follow up investigations (McManus et al., 2019; Muceli et al., 2022). Among these significant oscillation frequencies, the delta band of coherence (1-5 Hz) is believed to reflect the effective control signal to the motor neuron pool (i.e., voluntary component) as it encompasses the frequency range of the force signal (Farina et al., 2014). On the other hand, beta band oscillations (15-35 Hz) in motor unit coherence are commonly attributed to cortical origin, as studies have demonstrated associations between muscular and cortical activities within this frequency range (Conway et al., 1995b; Baker et al., 1997; Baker, 2007). Finally, the alpha band coherence (5-15 Hz) is usually associated with the physiological tremor originating from spinal reflex circuitry (i.e., involuntary component) (Conway et al., 1995a; Christakos et al., 2006; Laine et al., 2016). For instance, a demanding visuomotor task has been shown to increase alpha band coherence, which was accompanied by larger force tremors and H-reflex amplitudes (Laine et al., 2014). These findings, along with others (Ribot-Ciscar et al., 2009; Roche et al., 2011), suggest that a high-sensitivity task, such as the one presented to the participants in this study, decreases pre-synaptic inhibition of Ia afferents. This, in turn, would result in larger fluctuations in common synaptic noise in the alpha band and, consequently, lead to increased force oscillations. Indeed, as illustrated in **Figure 2A** and reflected in the coefficient of variation of force results, the *pre-skill acquisition* trial exhibited greater force fluctuations in both the TA and FDI muscles. Supporting this observation, we also found higher motor unit discharge variability, a measure of the variance of the common synaptic input received by the motor neurons, in the *pre-skill acquisition* trial (**Figures 3C** and **3D**), which is consistent with previous research (Knight and Kamen, 2004; Ely et al., 2022). However, we hypothesized that the repetition of this challenging task would prompt the central nervous system to effectively minimize the involuntary input components unrelated to the specific task. This would lead to reductions in alpha band oscillations (physiological tremor),

subsequent improvements in force control, and, ultimately, the short-term acquisition of the motor task.

We employed three complementary approaches to test our hypothesis. Firstly, we experimentally examined changes in motor unit coherence within delta, alpha and beta bands between *pre-* and *post-skill acquisition*. For both investigated muscles, our results revealed reductions in z-coherence, specifically within the physiological tremor frequency band (**Figure 4**), which supports our hypothesis. Secondly, we calculated the SNR between the target and the force, as well as between the target and the CST (an estimation of the effective neural drive to the muscle). We found that both the target-force and target-CST SNR values increased significantly with the skill acquisition (**Figure 5**), indicating a better match between the neural/mechanical outputs and the target task due to a decreased influence of involuntary unrelated noise oscillations. Finally, we conducted simulations that involved reducing the involuntary components of the shared synaptic input to the motor neuron pool while preserving the voluntary components. In all simulations, this reduction resulted in a significant decrease in alpha band coherence of the simulated motor neurons (**Figure 6**), which aligns with the experimental data obtained for both the FDI and TA muscles. Importantly, simulations with reduced involuntary synaptic input yielded lower errors between the simulated force output and the target, highlighting the pivotal role of decreased alpha band oscillations in the observed improvements in force-matching. These findings collectively support our hypothesis that the short-term acquisition of a force-matching skill involves a reduction of shared synaptic oscillations unrelated to the intended force output.

The observed decrease in alpha band oscillations could be attributed to modulations in spinal pathways, supraspinal pathways, or both. The possibility of spinal modulation aligns with

previous studies showing H-reflex depression following visuomotor skill tasks (Perez et al., 2005; Giboin et al., 2020), suggesting an increase in the presynaptic inhibition of Ia afferents during motor skill acquisition. Considering the involvement of Ia afferent loop in physiological tremor enhancement (Cresswell and Löscher, 2000; Christakos et al., 2006; Laine et al., 2016), this increased Ia inhibition with skill acquisition may underlie the reduction in physiological tremor oscillations. Additionally, neuroimaging evidence has demonstrated learning-related modulation of activity in the spinal region during the acquisition of a new motor skill (Vahdat et al., 2015). Therefore, alterations in the synaptic weights of Ia afferent activity arising from spinal pathways may provide a potential explanation for the observed outcomes in our study. At the cortical level, while alpha rhythm is more prominent in visual areas (Pfurtscheller et al., 1996), it can also be recorded above the sensory-motor cortical area (Pfurtscheller and Berghold, 1989). According to the alpha inhibition hypothesis (Klimesch, 1996; Pfurtscheller, 2001, 2003), alpha oscillations are thought to play an active role in top-down inhibitory control of neuronal processes and modulating cognitive functions such as perceptual learning (for a review, see Sigala et al. (2014)). Large-amplitude oscillations reveal the inhibition and disengagement of task-irrelevant cortical areas, whereas small alpha amplitudes are a signature of regions engaged in active cortical processing (for review, see Payne and Sekuler (2014)). Thus, the attenuation of alpha-band signals may reflect the gradual release of inhibition associated with the engagement of areas involved in complex processes of cortical activation (Klimesch et al., 2007). The changes in alpha band coherence observed in the present study at the neuromuscular level could be, at least in part, the expression of ongoing modulations in electrocortical brain activity transmitted to the motor neuron pools during the learning process of the visuomotor task. However, considering that in healthy individuals, cortico-muscular coherence does not show direct significant coherent oscillations in the alpha band (Conway et al., 1995b; Baker et al., 1997), we hypothesize that this modulated cortical activity could

indirectly influence the motor neuron pools through alterations in the pre-synaptic inhibition of Ia afferent activity. Therefore, as cognitive resources are increasingly engaged to tune the neural output (i.e., the cortical drive for muscular force) to task demands (i.e., force-matching improvement), there would be a reduction in the associated inhibition exerted toward the cortical areas (e.g., the motor cortex) under this top-down control. This reduction may potentially manifest as lower alpha band oscillations at the motor neuron pool level through changes in the weights of the pre-synaptic inhibitory pathways.

A final consideration on the shared synaptic alterations during the learning of a force-matching task is related to the lack of alterations in beta band oscillations. Our results showed no significant changes in beta band coherence between *pre-* and *post-skill acquisition* trials for both FDI and TA muscles (**Figure 4**). These results suggest that shared beta oscillations are unlikely to play a significant role in short-term acquisition of a force-matching skill task. This view is supported by recent research demonstrating no association between motor cortical beta power and learning during the execution of a complex sequential motor task (van der Cruijsen et al., 2021), and indicating that beta oscillations do not directly contribute to voluntary modulation of force (Zicher et al., 2022).

Finally, we observed a subtle increase in mean discharge rate (~1 pps; **Figures 3A** and **3B**) with the force-matching skill acquisition. An increase in mean discharge rate has been linked to improved transmission of common synaptic input to motor neuron spike trains (Negro and Farina, 2012), which would result in increased shared synaptic oscillations. Contrarily, we observed a decrease in shared synaptic noise oscillations despite the increase in mean discharge rate. Furthermore, we found no significant associations between changes in mean discharge rate and coherence across the evaluated frequency bands (see Spearman correlation results).

Taken together, these findings suggest that the observed increases in mean discharge rate are unlikely to explain the reductions in shared synaptic noise oscillations observed with force-matching skill acquisition. Thus, it is possible that changes in peripheral motor unit properties, such as reductions in motor unit twitch duration or amplitude, may have contributed to the observed changes in mean discharge rate. However, further investigation is warranted to elucidate the underlying mechanisms.

In conclusion, our study demonstrates that the acquisition of a force-matching skill involves specific adaptations in the shared synaptic input to alpha motor neurons, resulting in enhanced force control by minimizing shared noise oscillations unrelated to the task. These findings provide novel insights into the neural mechanisms underlying motor learning.

References

Baker SN (2007) Oscillatory interactions between sensorimotor cortex and the periphery. Current Opinion in Neurobiology 17:649-655.

Baker SN, Olivier E, Lemon RN (1997) Coherent oscillations in monkey motor cortex and hand muscle EMG show task-dependent modulation. J Physiol 501 (Pt 1):225-241.

Baker SN, Pinches EM, Lemon RN (2003) Synchronization in monkey motor cortex during a precision grip task. II. effect of oscillatory activity on corticospinal output. J Neurophysiol 89:1941-1953.

Baldissera F, Cavallari P, Cerri G (1998) Motoneuronal pre-compensation for the low-pass filter characteristics of muscle. A quantitative appraisal in cat muscle units. J Physiol 511 (Pt 2):611-627.

Bawa P, Stein RB (1976) Frequency response of human soleus muscle. J Neurophysiol 39:788-793.

Boccia G, Martinez-Valdes E, Negro F, Rainoldi A, Falla D (2019) Motor unit discharge rate and the estimated synaptic input to the vasti muscles is higher in open compared with closed kinetic chain exercise. J Appl Physiol (1985) 127:950-958.

Castronovo AM, Negro F, Conforto S, Farina D (2015) The proportion of common synaptic input to motor neurons increases with an increase in net excitatory input. J Appl Physiol (1985) 119:1337-1346.

Christakos CN, Papadimitriou NA, Erimaki S (2006) Parallel neuronal mechanisms underlying physiological force tremor in steady muscle contractions of humans. J Neurophysiol 95:53-66.

Cisi RR, Kohn AF (2008) Simulation system of spinal cord motor nuclei and associated nerves and muscles, in a Web-based architecture. J Comput Neurosci 25:520-542.

Cogliati M, Cudicio A, Martinez-Valdes E, Tarperi C, Schena F, Orizio C, Negro F (2020) Half marathon induces changes in central control and peripheral properties of individual motor units in master athletes. J Electromyogr Kinesiol 55:102472.

Conway BA, Farmer SF, Halliday DM, Rosenberg JR (1995a) On the Relation between Motor-Unit Discharge and Physiological Tremor. In: Alpha and Gamma Motor Systems (Taylor A, Gladden MH, Durbaba R, eds), pp 596-598. Boston, MA: Springer US.

Conway BA, Halliday DM, Farmer SF, Shahani U, Maas P, Weir AI, Rosenberg JR (1995b) Synchronization between motor cortex and spinal motoneuronal pool during the performance of a maintained motor task in man. J Physiol 489 (Pt 3):917-924.

Cresswell AG, Löscher WN (2000) Significance of peripheral afferent input to the alpha-motoneurone pool for enhancement of tremor during an isometric fatiguing contraction. Eur J Appl Physiol 82:129-136.

Dayan E, Cohen LG (2011) Neuroplasticity subserving motor skill learning. Neuron 72:443-454.

Ely IA, Jones EJ, Inns TB, Dooley S, Miller SBJ, Stashuk DW, Atherton PJ, Phillips BE, Piasecki M (2022) Training-induced improvements in knee extensor force accuracy are associated with reduced vastus lateralis motor unit firing variability. Experimental Physiology 107:1061-1070.

Enoka RM, Farina D (2021) Force Steadiness: From Motor Units to Voluntary Actions. Physiology 36:114-130.

Farina D, Negro F (2015) Common synaptic input to motor neurons, motor unit synchronization, and force control. Exerc Sport Sci Rev 43:23-33.

Farina D, Negro F, Dideriksen JL (2014) The effective neural drive to muscles is the common synaptic input to motor neurons. J Physiol 592:3427-3441.

Fuglevand AJ, Winter DA, Patla AE (1993) Models of recruitment and rate coding organization in motor-unit pools. J Neurophysiol 70:2470-2488.

Gallet C, Julien C (2011) The significance threshold for coherence when using the Welch's periodogram method: Effect of overlapping segments. Biomedical Signal Processing and Control 6:405-409.

Giboin L-S, Tokuno C, Kramer A, Henry M, Gruber M (2020) Motor learning induces time-dependent plasticity that is observable at the spinal cord level. The Journal of Physiology 598:1943-1963.

Hassan A, Thompson CK, Negro F, Cummings M, Powers RK, Heckman CJ, Dewald JPA, McPherson LM (2020) Impact of parameter selection on estimates of motoneuron excitability using paired motor unit analysis. J Neural Eng 17:016063.

Heathcote A, Brown S, Mewhort DJK (2000) The power law repealed: The case for an exponential law of practice. Psychonomic Bulletin & Review 7:185-207.

Hug F, Avrillon S, Del Vecchio A, Casolo A, Ibanez J, Nuccio S, Rossato J, Holobar A, Farina D (2021) Analysis of motor unit spike trains estimated from high-density surface electromyography is highly reliable across operators. J Electromyogr Kinesiol 58:102548.

Jensen JL, Marstrand PC, Nielsen JB (2005) Motor skill training and strength training are associated with different plastic changes in the central nervous system. J Appl Physiol (1985) 99:1558-1568.

Johansson RS, Westling G (1988) Programmed and triggered actions to rapid load changes during precision grip. Exp Brain Res 71:72-86.

Kapelner T, Sartori M, Negro F, Farina D (2020) Neuro-Musculoskeletal Mapping for Man-Machine Interfacing. Scientific Reports 10:5834.

Karni A, Meyer G, Jezzard P, Adams MM, Turner R, Ungerleider LG (1995) Functional MRI evidence for adult motor cortex plasticity during motor skill learning. Nature 377:155-158.

Karni A, Meyer G, Rey-Hipolito C, Jezzard P, Adams MM, Turner R, Ungerleider LG (1998) The acquisition of skilled motor performance: Fast and slow experience-driven changes in primary motor cortex. Proceedings of the National Academy of Sciences 95:861-868.

Kleim JA, Barbay S, Nudo RJ (1998) Functional reorganization of the rat motor cortex following motor skill learning. J Neurophysiol 80:3321-3325.

Klimesch W (1996) Memory processes, brain oscillations and EEG synchronization. Int J Psychophysiol 24:61-100.

Klimesch W, Hanslmayr S, Sauseng P, Gruber WR, Doppelmayr M (2007) P1 and Traveling Alpha Waves: Evidence for Evoked Oscillations. Journal of Neurophysiology 97:1311-1318.

Knight CA, Kamen G (2004) Enhanced motor unit rate coding with improvements in a force-matching task. Journal of Electromyography and Kinesiology 14:619-629.

Kumar A, Tanaka Y, Grigoriadis A, Grigoriadis J, Trulsson M, Svensson P (2017) Training-induced dynamics of accuracy and precision in human motor control. Scientific Reports 7:6784.

Kuznetsova A, Brockhoff PB, Christensen RHB (2017) lmerTest Package: Tests in Linear Mixed Effects Models. Journal of Statistical Software 82:1 - 26.

Laine CM, Yavuz SU, Farina D (2014) Task-related changes in sensorimotor integration influence the common synaptic input to motor neurones. Acta Physiol (Oxf) 211:229-239.

Laine CM, Nagamori A, Valero-Cuevas FJ (2016) The Dynamics of Voluntary Force Production in Afferented Muscle Influence Involuntary Tremor. Front Comput Neurosci 10:86.

Lenth R, Singmann H, Love J, Buerkner P, Herve M (2019) Package ‘emmeans’. In.

Maillet J, Avrillon S, Nordez A, Rossi J, Hug F (2022) Handedness is associated with less common input to spinal motor neurons innervating different hand muscles. J Neurophysiol 128:778-789.

Martinez-Valdes E, Negro F, Laine CM, Falla D, Mayer F, Farina D (2017) Tracking motor units longitudinally across experimental sessions with high-density surface electromyography. J Physiol 595:1479-1496.

Mazzo MR, Weinman LE, Giustino V, McLagan B, Maldonado J, Enoka RM (2021) Changes in neural drive to calf muscles during steady submaximal contractions after repeated static stretches. J Physiol 599:4321-4336.

McManus L, Flood MW, Lowery MM (2019) Beta-band motor unit coherence and nonlinear surface EMG features of the first dorsal interosseous muscle vary with force. J Neurophysiol 122:1147-1162.

Muceli S, Poppendieck W, Holobar A, Gandevia S, Liebetanz D, Farina D (2022) Blind identification of the spinal cord output in humans with high-density electrode arrays implanted in muscles. Science Advances 8:eabo5040.

Negro F, Farina D (2011a) Linear transmission of cortical oscillations to the neural drive to muscles is mediated by common projections to populations of motoneurons in humans. J Physiol 589:629-637.

Negro F, Farina D (2011b) Decorrelation of cortical inputs and motoneuron output. J Neurophysiol 106:2688-2697.

Negro F, Farina D (2012) Factors influencing the estimates of correlation between motor unit activities in humans. PLoS One 7:e44894.

Negro F, Holobar A, Farina D (2009) Fluctuations in isometric muscle force can be described by one linear projection of low-frequency components of motor unit discharge rates. J Physiol 587:5925-5938.

Negro F, Yavuz U, Farina D (2016a) The human motor neuron pools receive a dominant slow-varying common synaptic input. J Physiol 594:5491-5505.

Negro F, Muceli S, Castronovo AM, Holobar A, Farina D (2016b) Multi-channel intramuscular and surface EMG decomposition by convolutive blind source separation. J Neural Eng 13:026027.

Nudo RJ, Milliken GW, Jenkins WM, Merzenich MM (1996) Use-dependent alterations of movement representations in primary motor cortex of adult squirrel monkeys. J Neurosci 16:785-807.

Oliveira AS, Negro F (2021) Neural control of matched motor units during muscle shortening and lengthening at increasing velocities. J Appl Physiol (1985) 130:1798-1813.

Pascual-Leone A, Tarazona F, Catalá MD (1999) Applications of transcranial magnetic stimulation in studies on motor learning. Electroencephalogr Clin Neurophysiol Suppl 51:157-161.

Pascual-Leone A, Nguyet D, Cohen LG, Brasil-Neto JP, Cammarota A, Hallett M (1995) Modulation of muscle responses evoked by transcranial magnetic stimulation during the acquisition of new fine motor skills. J Neurophysiol 74:1037-1045.

Payne L, Sekuler R (2014) The importance of ignoring: Alpha oscillations protect selectivity. Curr Dir Psychol Sci 23:171-177.

Perez MA, Lungholt BKS, Nielsen JB (2005) Presynaptic control of group Ia afferents in relation to acquisition of a visuo-motor skill in healthy humans. The Journal of Physiology 568:343-354.

Perez MA, Lungholt BK, Nyborg K, Nielsen JB (2004) Motor skill training induces changes in the excitability of the leg cortical area in healthy humans. Exp Brain Res 159:197-205.

Pfurtscheller G (2001) Functional brain imaging based on ERD/ERS. Vision Res 41:1257-1260.

Pfurtscheller G (2003) Induced oscillations in the alpha band: functional meaning. Epilepsia 44 Suppl 12:2-8.

Pfurtscheller G, Berghold A (1989) Patterns of cortical activation during planning of voluntary movement. Electroencephalogr Clin Neurophysiol 72:250-258.

Pfurtscheller G, Stancák A, Neuper C (1996) Event-related synchronization (ERS) in the alpha band — an electrophysiological correlate of cortical idling: A review. International Journal of Psychophysiology 24:39-46.

Plautz EJ, Milliken GW, Nudo RJ (1995) Differential effects of skill acquisition and motor use on the reorganization of motor representations in area 4 of adult squirrel monkeys. . In: Society for Neuroscience.

Ribot-Ciscar E, Hospod V, Roll JP, Aimonetti JM (2009) Fusimotor drive may adjust muscle spindle feedback to task requirements in humans. J Neurophysiol 101:633-640.

Roche N, Bussel B, Maier MA, Katz R, Lindberg P (2011) Impact of precision grip tasks on cervical spinal network excitability in humans. The Journal of Physiology 589:3545-3558.

Rossato J, Tucker K, Avrillon S, Lacourpaille L, Holobar A, Hug F (2022) Less common synaptic input between muscles from the same group allows for more flexible coordination strategies during a fatiguing task. J Neurophysiol 127:421-433.

Sigala R, Haufe S, Roy D, Dinse HR, Ritter P (2014) The role of alpha-rhythm states in perceptual learning: insights from experiments and computational models. Front Comput Neurosci 8:36.

Tenan MS, Marti CN, Griffin L (2014) Motor unit discharge rate is correlated within individuals: a case for multilevel model statistical analysis. J Electromyogr Kinesiol 24:917-922.

Thompson CK, Negro F, Johnson MD, Holmes MR, McPherson LM, Powers RK, Farina D, Heckman CJ (2018) Robust and accurate decoding of motoneuron behaviour and prediction of the resulting force output. J Physiol 596:2643-2659.

Ungerleider LG, Doyon J, Karni A (2002) Imaging brain plasticity during motor skill learning. Neurobiol Learn Mem 78:553-564.

Vahdat S, Lungu O, Cohen-Adad J, Marchand-Pauvert V, Benali H, Doyon J (2015) Simultaneous Brain–Cervical Cord fMRI Reveals Intrinsic Spinal Cord Plasticity during Motor Sequence Learning. PLOS Biology 13:e1002186.

van der Cruijsen J, Manoochehri M, Jonker ZD, Andrinopoulou E-R, Frens MA, Ribbers GM, Schouten AC, Selles RW (2021) Theta but not beta power is positively associated with better explicit motor task learning. NeuroImage 240:118373.

Willingham DB (1998) A neuropsychological theory of motor skill learning. Psychol Rev 105:558-584.

Zicher B, Ibáñez J, Farina D (2022) Beta inputs to motor neurons do not directly contribute to volitional force modulation. J Physiol.